

Magnetic behaviour and microstructural properties of amorphous and crystallized $Y_{3-x}Gd_xFe_5O_{12}$ prepared by the amorphous citrate process ($x = 0, 0.5$ and 3)

D. ROY, R. BHATNAGAR, D. BAHADUR

Advanced Centre for Materials Science, Indian Institute of Technology, Kanpur, 208016, India

The systems $Y_{3-x}Gd_xFe_5O_{12}$ with $x = 0, 0.5$ and 3 have been synthesized by the amorphous citrate process. Their structural and magnetic properties have been studied for various heat-treatment schedules. The systems with $x = 0, 0.5$ and 3 are amorphous when heat treated up to $650, 600$ and 500°C , respectively, and the results of amorphous, as well as crystallized, samples are discussed. The volume fraction of the garnet phase is found to increase with higher heat-treatment temperature. Besides the garnet phase, two other phases appear to grow, the volume fraction of the spinel phase increasing with increase in gadolinium concentration. Microstructural properties have been further correlated with the magnetic properties.

1. Introduction

To fulfil the requirements for a fast solid state reaction, some specialized preparative techniques such as freeze drying [1], the gel process [2] and the amorphous citrate process [3, 4] have been tried out in recent years. Among these, the last is believed to have great potential. Non-crystalline yttrium iron garnet has been prepared by different methods and characterized [5-8]. The amorphous citrate process has also been used to produce yttrium iron garnet [9].

The present study describes an attempt to synthesize the systems $Y_{3-x}Gd_xFe_5O_{12}$ ($x = 0, 0.5$ and 3) by the amorphous citrate process. Their magnetic behaviour and microstructural properties have been investigated before and after crystallization. The temperature for amorphous to crystalline transformation has been determined. Different heat treatments have been given and the resultant crystallized or amorphous phases have been characterized in detail using X-ray, thermogravimetry analysis, electron microscopy and magnetic measurements. The results are presented here.

2. Experimental details

The materials were prepared from analytical grade chemicals. The stoichiometric amounts of Y_2O_3 and Gd_2O_3 were dissolved in 5N HNO_3 . The solution was evaporated to dryness. The dried solid was redissolved in water. The required amounts of ferric citrate and citric acid solution in water were added. Citric acid was added in excess. The mixture was refluxed for about 6h. The refluxed solution was kept at 120°C for drying. Two different heat-treatment schedules were given for the dried precursors. In the first schedule, the obtained product was heated at 400°C for 24h in an atmosphere of 95% nitrogen and 5% oxygen and again for 24h at 400°C in air. This was followed by heating in air at different temperatures for 4h each. In the other heating schedule, the initial heat treatment at 400°C was given only in air instead of in a mixture of nitrogen and oxygen. These heating schedules will be referred in the text as N and A, respectively. All the products obtained are given in Table I. X-ray diffractograms were taken with a Rich Seifert Iso-debyeflex 2002 diffractometer. Thermo-

TABLE I Details of the samples studied. All samples heat treated for 4 h (temperature in °C).

System	Samples given heat schedule A						Samples given heat schedule N			
	400	500	600	700	800	900	500	600	650	700
$x = 0.0$	YA4	YA5	YA6	YA7	YA8	YA9		YN6	YN6.5	YN7
$x = 0.5$	YGA4		YGA6	YGA7	YGA8			YGN6	YGN6.5	YGN7
$x = 3$							GN5	GN6		GN7

gravimetry analysis was performed using a MOM Hungary Derivatograph. Magnetic measurements were obtained with a PAR 150 vibrating sample magnetometer in conjunction with a Varian magnet. Electron micrographs were taken with a Philips TEM 301 transmission electron microscope.

3. Results and discussion

The systems $Y_{3-x}Gd_xFe_5O_{12}$ are X-ray amorphous when heated at ≤ 650 , 600 and 500°C for $x = 0$, 0.5 and 3, respectively. The samples which are amorphous, show evidence of phase separation. A typical electron micrograph for the sample YGA6 is shown in Fig. 1. The transition temperature for crystallization decreases with increase in gadolinium substitution. Thermogravimetry data show that the citrate mixture decomposes into constituent oxides up to 500°C, above which the weight loss is small. We will first discuss the system with $x = 0$ in detail and follow it by systems with $x = 0.5$ and 3.

3.1. $x = 0$

The X-ray data of the various heat-treated samples (which are crystallized) are given in Table II. X-ray data indicate that the major crystalline phase is

yttrium iron garnet. However, there are a few extra lines which could not be indexed for the YIG phase. This could be due to a small volume fraction of some other phases. Since, our main interest was in the YIG phase, we have not gone into detailed analysis of the other phases present. The extra lines in the X-ray diffraction pattern could not be indexed due to a single phase. There is clear evidence of α - Fe_2O_3 phase. Besides this, there are lines due to the spinel phase which could be assigned to γ - Fe_2O_3 or Fe_3O_4 .

Heat schedule A seems to be more favourable for the growth of the garnet phase. Further heat treatment at higher temperatures is more favourable for this phase. The results obtained through X-ray diffraction studies are also supported by electron diffraction and microscopic studies. The samples in their amorphous region show evidence of more than one phase, which is obvious from electron microscopic studies. The presence of more than one phase is also evident from magnetization studies. A plot of magnetization against temperature between 300 and 900 K (at a field of 6 kG) for the samples YA6, YA7 and YN7 is shown in Fig. 2. The inset shows the same plot in a residual field for the samples YA7 and YA8. In order to obtain idea of the behaviour below room temperature, measurements were made up to 77 K for sample YN7 only, and this plot is included in Fig. 2. Since there was nothing unexpected, we did not repeat this measurement for the other samples. The plot in Fig. 2 shows an obvious transition at around 550 K which is the Curie temperature for yttrium iron garnet. The final transition beyond which these samples are paramagnetic is around 875 K. This transition is typical of a spinel phase. The transition due to α - Fe_2O_3 may not be evident because of its canted antiferromagnetic structure. There is essentially only one transition for the sample YA7. The plot in the inset is indicative of only one transition at 550 K for the garnet phase. The difference in behaviour below 475 K, between the two samples (given in the inset) is not clearly understood at present.

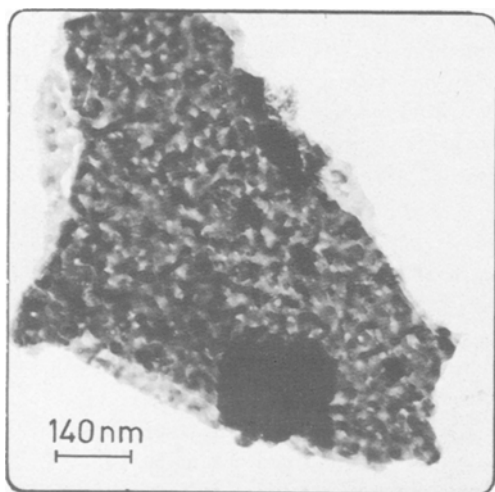


Figure 1. A typical electron micrograph for sample YGA6.

TABLE II X-ray data for the sample with $x = 0$

YA7		YN7		YA8		YA9		Assignment, phase*, hkl
d (nm)	I/I_0	d (nm)	I/I_0	d (nm)	I/I_0	d (nm)	I/I_0	
0.3413	32					0.3421	14	S(211)
0.3083	40	0.3089	43	0.3082	59	0.3063	30	G(400)
0.297	10	0.2960	84	0.2954	35			S(220)
0.2761	82	0.2772	58	0.2778	100	0.2761	100	G(420)
0.2684	100	0.2709	100	0.2694	100	0.2699	70	H(104)
0.2522	60	0.2552	31	0.2522	57	0.2517	47	G(422), S(311), H(110)
0.2471	29	0.2426	21	0.2430	34	0.2432	12	S(222)
0.2262	33			0.2263	32	0.2256	17	G(521)
0.211	28	0.2119	33	0.2105	30	0.2113	11	S(400)
0.2016	22	0.2034	20	0.2008	23	0.205	15	G(611,532)
0.1941	34	0.1943	21			0.1943	15	
0.1898	47			0.1896	23			S(420)
0.1853	29	0.1865	28	0.1855	25	0.1825	16	H(024)
0.1790	22	0.1785	29	0.1783	22			G(444)
0.1716	34	0.1724	54	0.1719	27	0.1716	33	G(640)
0.1654	17	0.1657	21	0.1654	55	0.1651	15	G(642)
0.1604	19	0.1626	28	0.1629	47	0.1630	10	H(211), S(511,333)
0.1572	25	0.1581	24			0.1586	17	G(732,651), H(018)
0.1544	35	0.1540	20	0.1533	23			G(800)
0.1489	16	0.1499	25	0.1498	27			S(440)

*G = garnet phase, S = spinel phase, H = hexagonal phase.

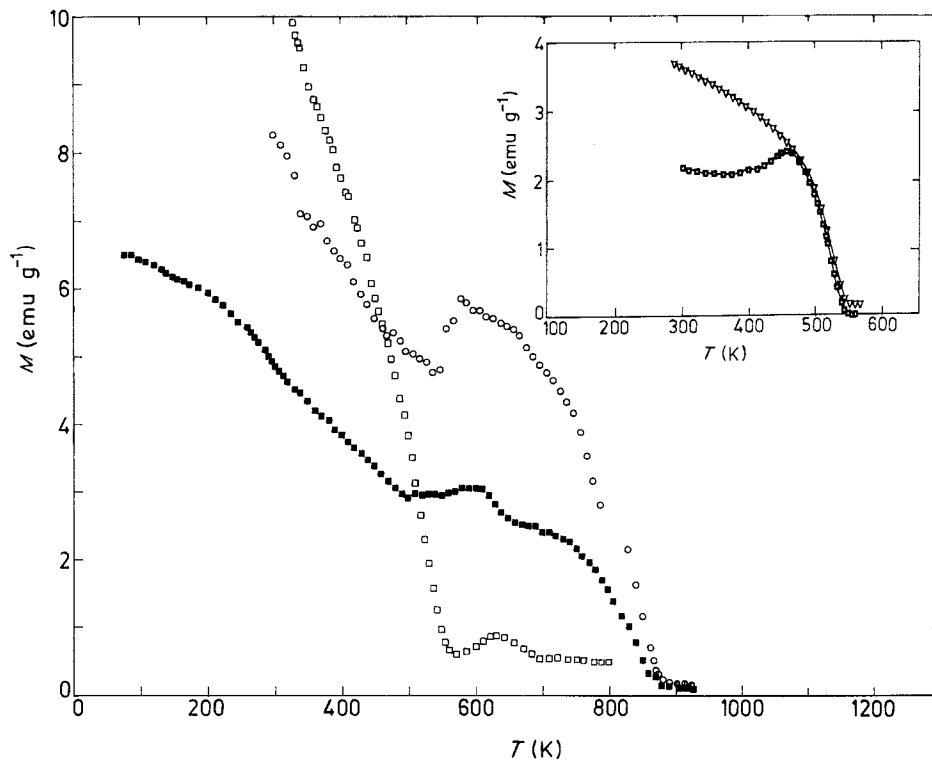


Figure 2. Plot of magnetic moment against temperature (at a field of 6 kG) for different samples with $x = 0$. The inset shows the same plot in the residual field. (\circ YA6; \square YA7; ∇ YA8; \blacksquare YN7.)

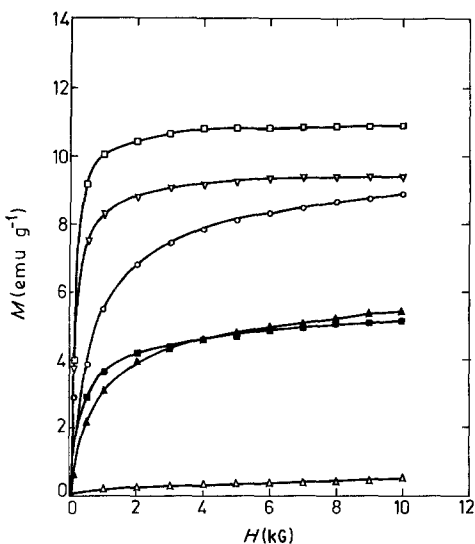


Figure 3. Plot of magnetic moment against magnetic field for different samples with $x = 0$. (Δ YA4; \circ YA6; \square YA7; ∇ YA8; \blacktriangle YN6.5; \blacksquare YN7.)

However, as evident from X-ray data, the growth of different phases essentially depends upon the heat-treatment schedule and the behaviour could depend upon the ratio of different phases present. If we compare samples YA7 and YN7 for which the heat-treatment temperature and time are identical, but the atmosphere of heating is different, we observe that heat schedule A is more favourable for the garnet phase. X-ray and electron diffraction data also support this behaviour.

To obtain further insight into the magnetic behaviour, we have plotted magnetization against field for various samples in Fig. 3. The sample YA4 essentially shows a paramagnetic behaviour with a very low moment. Samples YA6, YN6.5 and YN7 do not saturate up to a field of 10 kG. However, samples YA7 and YA8 show evidence of saturation. The absence of saturation in the former samples could be due to variation in particle size and superparamagnetic behaviour of the particles [5, 6, 10]. Variation in particle size is further evident from electron micrographs. The absence of saturation could also be due to the presence of α - Fe_2O_3 as the major crystalline phase. This being canted antiferromagnetic, may result in such a behaviour. In Fig. 3, it is also observed that there is no systematic behaviour of saturation moments as against the heating schedules. This is probably due to the different heating schedules which give rise to the growth of different phases in different ratios.

Considering all the X-ray and magnetic data, it appears that heating in air and at high temperature is more favourable for the growth of the garnet phase. Fig. 3 gives the highest saturation moment for the sample YA7. The corresponding $4\pi Ms$ value is estimated as 855 G. The value of $4\pi Ms$ for the polycrystalline YIG sample is reported to be around 1750 G at room temperature [11]. The large discrepancy in $4\pi Ms$ value appears to be due to the presence of other phases such as α - Fe_2O_3 possessing lower moments. It could also be due to the effect of particle size.

3.2. $x = 0.5$

This sample, as mentioned earlier, is amorphous for the heat-treatment temperature of $\leq 600^\circ\text{C}$. X-ray data of the heat-treated samples show essentially the same behaviour as for $x = 0$. Heat schedule A followed by heat treatment at higher temperatures appears to be more favourable for the growth of the garnet phase. Besides this, some other phases such as α - Fe_2O_3 and the spinel phase may also be present as is evident from X-ray data. The ratio of these phases present is dependent upon the heat schedule used, as is observed for $x = 0$.

Plots of magnetization against field for various heat-treated samples are given in Fig. 4. The samples YGN6 and YGN6.5 do not saturate whereas the samples YGN7, YGA7 and YGA8 show saturation effects. This is similar to the behaviour for samples with $x = 0$. Among the saturated samples, the sample YGA8 shows the largest saturation moment. The corresponding $4\pi Ms$ value obtained is 1600 G which is very close to the literature value [11]. The $4\pi Ms$ values obtained for samples YGA7 and YGN7 are 1270 and 1100 G, respectively. The slight reduction could be due to the presence of a certain fraction of other phases present, and also because of variation in the particle size. From this plot, it appears that sample YGA8 contains the maximum amount of the garnet phase. This is also supported by X-ray data which exhibit stronger X-ray diffraction lines due to the garnet phase.

To obtain further insight into possible phases present and their magnetic behaviour, we have plotted the magnetization (at a field of 6 kG) against temperature for samples YGA6, YGN6.5 and YGN7 in Fig. 5. We have selected only those samples for which the heat-treatment temperatures are in the vicinity of the crystallization tempera-

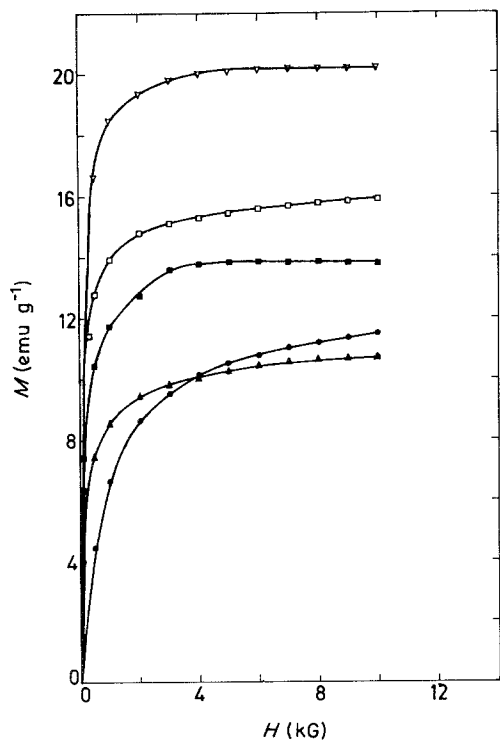


Figure 4. Plot of magnetic moment against magnetic field for different samples with $x = 0.5$. (\square YGA7; ∇ YGA8; \bullet YGN6; \blacktriangle YGN6.5; \blacksquare YGN7.)

ture. In the inset we have given the plot of magnetization against temperature in the residual field for the two well-crystallized samples YGA7 and YGA8.

Ferrimagnetic interactions are evident from these plots. Furthermore, these plots (at 6 kG) indicate the presence of at least one more phase other than the garnet phase. The Curie temperature of the garnet phase, as estimated from these plots, is 550 K. The Curie temperature of the other possible phase is once again around 875 K indicating the presence of the spinel phase. The proportion of this phase decreases as the heat-treatment temperature increases. This is obvious from Fig. 5 where the sample YGN7 does not show any evidence of spinel phase. However, a small fraction of the spinel phase is present as is evident from the X-ray data. The data for sample YGN6.5 show the presence of a small fraction and those for YGA6 show a rather large fraction. A similar observation has been made from the X-ray data for samples YGA7 and YGN6.5. In order to see whether the magnetization behaviour is similar to that reported for polycrystalline gadolinium-substituted YIG, measurements for YGN7 were taken up to 77 K and the data are included in the same figure. It is

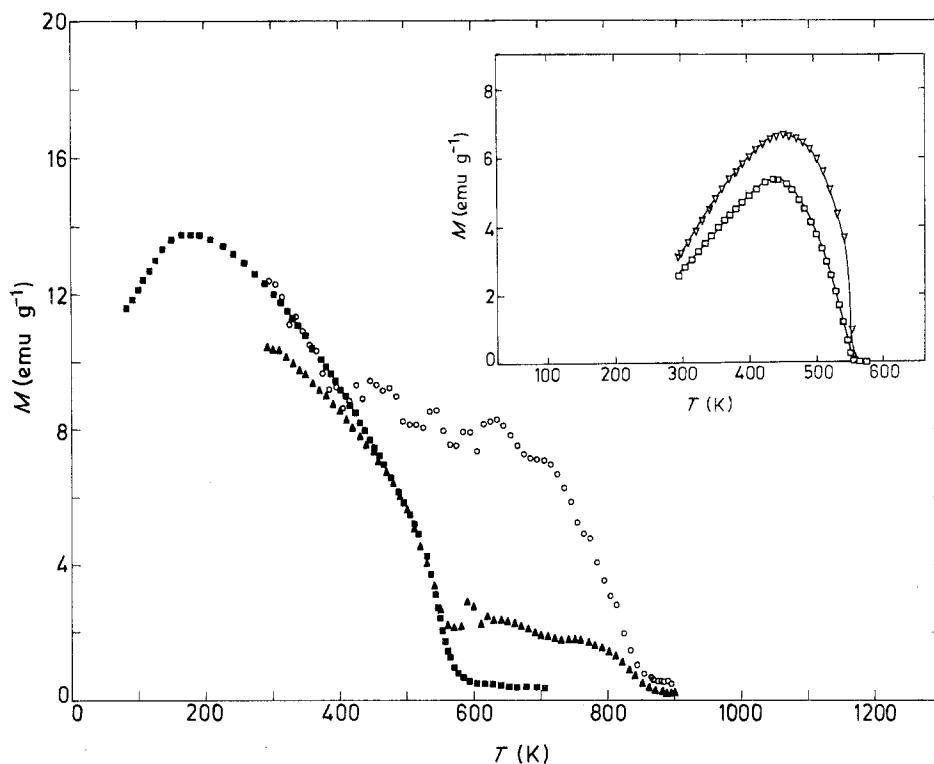


Figure 5. Plot of magnetic moment against temperature (at a field of 6 kG) for different samples with $x = 0.5$. The inset shows the plot in a residual field. (\circ YGA6; \blacktriangle YGN6.5; \blacksquare YGN7; \square YGA7; ∇ YGA8.)

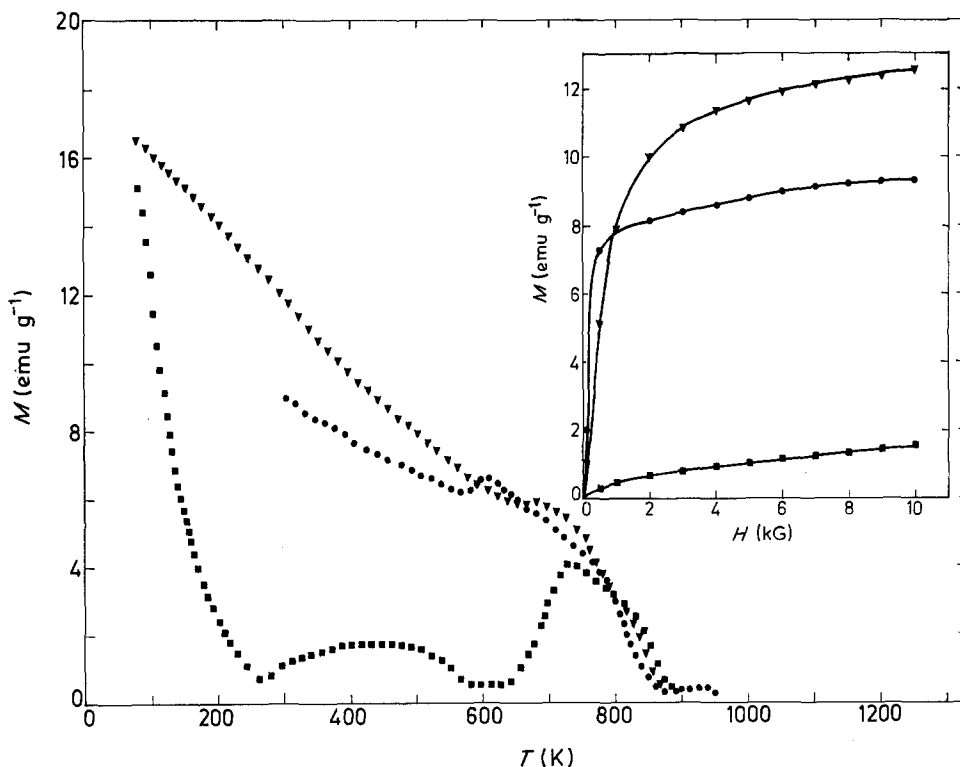


Figure 6. Plot of magnetic moment against temperature (at a field of 6 kG) for different samples with $x = 3$. The inset shows the plot of magnetic moment against magnetic field. (\blacktriangledown GN5; \bullet GN6; \blacksquare GN7.)

interesting to find this behaviour similar to that reported in the literature for polycrystalline samples [11]. Furthermore, the value of $4\pi Ms$ obtained for YGN7 at 77 K is 1020 G whereas this value is 1100 G at room temperature. This trend is consistent with that reported for polycrystalline samples [11].

3.3. $x = 3$

This sample is amorphous up to the heat-treatment temperature of $\leq 500^\circ\text{C}$. X-ray data of all the crystallized samples indicate the presence of the garnet phase, the proportion of which increases as the heat-treatment temperature increases. As found in the case of the two previous samples, this sample also exhibits the presence of other phases besides the garnet phase. For this sample, only heat schedule N is used. It is remarkable that the X-ray diffraction lines (other than those due to the garnet phase) found for this sample, are nearly the same as those observed for the other two samples.

Magnetic data for the various heat-treated samples are given in Fig. 6 as the plot of magnetization against temperature. The inset shows the plot of magnetization against field. The data of

magnetization against temperature have been at a field of 6 kG between 77 and 900 K for GN5 and GN7 whereas for GN6, it is between 300 and 900 K. Sample GN7, for which the X-ray data indicate the maximum amount of GdIG phase, shows a compensation temperature around 275 K as observed for polycrystalline GdIG [11]. The Curie temperature of the polycrystalline GdIG is around 560 K which is also exhibited by this sample. However, there is another transition around 875 K similar to that found for the previous two systems. This could be due to the spinel phase. X-ray lines due to this phase are also present in these samples. We have not observed a compensation temperature for samples GN5 and GN6. This is probably due to the presence of a large amount of spinel phase which overshadows the compensation temperature. The Curie temperature of the garnet phase is, however, indicated by a change in slope around 560 K. The transition at 875 K is clearer in these samples. This is again indicative of a large proportion of spinel phase in these samples. Substitution of Gd^{3+} for Y^{3+} results in exsolution of the spinel phase which increases with the concentration of Gd^{3+} ion. Magnetic and

TABLE III Magnetic data and particle size determined by different methods.

Sample	Magnetic data (G)				Particle size (nm)		
	300 K		77 K		<i>M-H</i> plot	EM	XRD
	<i>H_c</i>	<i>M_s</i>	<i>H_c</i>	<i>M_s</i>			
YA6	10	45	45	100	48.5	8	3
YA7	25	70				25.5	33
YA8	25	55					
YN6.5	25	30*					
YN7	20	85*	30	45			
YGA7	35	100					
YGA8	35	130					
YGN6	0	49*	30	55	43.5	13.5	4
YGN6.5	24	55*					
YGN7	40	85	115	80		60	40
GN5	0	100*			52.5	66.5	6.5
GN6	25	75*				77	45
GN7	100	10*		140			

*These values are for spontaneous magnetization at 10 kG field.

X-ray data support this behaviour. The size of the substituting rare earth ion is a predominant factor for the exsolution of the spinel phase [12].

A plot of *M* against *H* at room temperature, shown in the inset of Fig. 6, indicates that none of these samples becomes saturated even up to a field of 10 kG. This may be ascribed to the presence of superparamagnetic particles or to the presence of a canted antiferromagnetic phase such as α -Fe₂O₃. Another interesting feature of this plot is the value of spontaneous magnetization at room temperature which decreases as the heat-treatment temperature increases. This is possible as the compensation temperature of the GdIG phase is just below room temperature. Hence, as the heat-treatment temperature increases, the amount of garnet phase formed is greater. Therefore, the resultant magnetic moment decreases.

It is essential to have an understanding of the relative magnetic and microstructural properties of the three samples, presently studied. A discussion of this aspect is in order here. Table III lists the saturation magnetization or the spontaneous magnetization as the case may be, the coercive field and the average particle size determined by three different methods for various samples [13–15]. The particle size has been obtained from (a) the plot of magnetization against field, (b) X-ray line broadening, and (c) electron micrographs. Since our main intention was to obtain a qualitative idea of the particle size and its distribution in both crystalline and non-crystalline samples, measurements were taken only for one each of

the amorphous and crystalline samples. For amorphous samples, the particle size obtained by X-ray line broadening appears to be more reliable. The difference with the other two measurements could be explained assuming that the effective particle size obtained by these methods could be due to agglomeration of smaller particles or particle size distribution which has not been taken into account. In general, the particle size appears to increase with gadolinium substitution. It has been pointed out that the requirement for heat-treatment temperature for crystallization decreases as the gadolinium content increases.

The magnetic data have already been discussed individually for each sample. For amorphous samples such as YA6, YGN6 and GN5, the coercivity and remanence are nearly zero indicating superparamagnetic behaviour. The data for well-crystallized samples in each case show a clear evidence of the garnet phase as the major phase. However, the other phases such as α -Fe₂O₃ and the spinel phase are also present in smaller proportions; the proportions of these phases are large in amorphous samples as is evident from X-ray and magnetic data. The proportion of the spinel phase increases as the gadolinium concentration increases [12]. The volume fraction of the spinel and hexagonal phases varies depending upon the composition and conditions [10, 16, 17]. In fact, the coexistence of different oxidation products of iron is quite common and their relative concentration is dependent on the conditions and the presence of hydrogen ions.

Acknowledgement

We wish to thank the Department of Atomic Energy, Government of India, for financial support.

References

1. D. W. JOHNSON and F. J. SCHNEETTLER, *J. Amer. Ceram. Soc.* **53** (1970) 440.
2. A. C. C. TSEUNG and H. L. BEVAN, *J. Mater. Sci.* **5** (1970) 604.
3. D. J. ANDERSON and F. R. SALE, *Powder Metal.* **22** (1979) 14.
4. M. S. G. BAYTHORN and F. R. SALE, *J. Mater. Sci.* **17** (1982) 2757.
5. AKHILESH PRASAD, D. BAHADUR, R. M. SINGRU and D. CHAKRAVORTY, *ibid.* **17** (1982) 2687.
6. D. BAHADUR, P. K. DAS and D. CHAKRAVORTY, *J. Appl. Phys.* **53** (1982) 7813.
7. E. SAWATZKY and E. KAY, *ibid.* **39** (1968) 4700.
8. D. BAHADUR and K. N. RAI, *Mater. Res. Bull.* **15** (1980) 501.
9. TH. J. A. POPMA and A. M. VANDIEPEN, *ibid.* **9** (1974) 1119.
10. G. BATE, "Ferromagnetic Materials," Vol II, edited by E. P. Wohlfarth (North Holland, New York, 1980).
11. W. H. VON AULOCK, "Handbook of Microwave Ferrite Materials" (Academic Press, New York, 1965).
12. J. Y. LAVAL, *J. Amer. Ceram. Soc.* **61** (1978) 455.
13. S. DUTTA, D. BAHADUR and D. CHAKRAVORTY, *J. Phys. D Appl. Phys.* **17** (1984) 163.
14. J. J. BECKER, *J. Met.* **9** (1957) 59.
15. B. D. CULLITY, "Elements of X-ray Diffraction" (Addison Wesley, New York, 1978).
16. T. ELDER, *J. Appl. Phys.* **36** (1965) 1012.
17. AKHILESH PRASAD, R. M. SINGRU, D. BAHADUR and D. CHAKRAVORTY, *J. Mater. Sci.* (1984).

Received 17 November 1983
and accepted 13 March 1984